Forest Fire Susceptibility Mapping of West Sikkim District, India using MCDA techniques of AHP & TOPSIS model

Suvankar Naskar
Mizoram University
Aneesah Rahaman
University of Madras
Brototi Biswas (brototibiswas@gmail.com)
Mizoram University

Research Article

Keywords: forest fire, susceptibility, GIS, AHP, TOPSIS, AUC

Posted Date: June 23rd, 2022

DOI: https://doi.org/10.21203/rs.3.rs-1753672/v1

Abstract

Forest fire poses major environmental hazard, to the extent of sometimes permanently damaging the forest ecology. The potential of human to repair nature is hampered by the extension of human domination into forests, which results in the loss of forest land. While human expansion cannot be stopped, we must accept responsibility for the consequences and thus work to minimize such environmental hazards emanating from such calamities. RS and GIS have proved to be useful techniques for such studies. The goal of the current study is to identify the most vulnerable forest fire zones in the West Sikkim district falling within the state of Sikkim (India) during 2004–2021. Various thematic layers (LULC and topographical factors) were created using Landsat 8 OLI and ASTER DEM. For the final forest fire susceptibility zone (FFSZ) map, climate variables such as precipitation, temperature, humidity, and wind speed were also used. The authors employed the MCDM techniques of AHP and TOPSIS to determine the areas which are most vulnerable to wildfires in the research area. 194 wildfire locations, as obtained from Sikkim State Disaster Management Authority (SDMA) were used for the classification. The FFSZ were classified as “very high, high, medium, low, and very low vulnerability zones” based on their fire vulnerability. The areas under “Very high Susceptibility Zone” of AHP and TOPSIS were 152.331 km^2 and 348.499 km^2 respectively whereas the areas under “Very Low Susceptibility Zone” were 115.351 km^2 and 139.436 km^2 in the results of AHP and TOPSIS respectively. To check the accuracy of the FFSZ susceptibility maps obtained from the two modeling techniques, the same were confirmed by using (Receiver Operating Characteristics) ROC curves. Result indicates that the TOPSIS model (AUC = 82.28%) is slightly better at determining the vulnerable zones than the AHP method (AUC = 72.25%). Use of Geo-spatial technology can be an effective tool for delineating forest fire-prone areas of West Sikkim district. A fire risk map is useful for preventing possible tragedies by allowing and planning of enough fire-fighting infrastructures in areas vulnerable to fire damage.

1. Introduction

Forest fire is among nature's most fundamental disturbance factors, and is responsible for landscape modification and vegetation succession (E. Chuvieco and J. Salas 1996). Forest fire results in soil erosion, land degradation, increased CO_2 emissions, alteration in species diversity, etc. (Borrelli et al. 2017). It has major economic consequences on public property, while also posing risk to human life, once they advance to populated areas. Research findings show that forest fires disrupt ecological equilibrium and amplify the greenhouse effect (Mikhaylov et al. 2020; Sannigrahi et al. 2020). Huge amounts of aerosol contaminants are generated during fires, affecting the chemical structure, lowering the quality of air and jeopardizing human health (Rongbin et al. 2020). Soil erosion, floods, variations in the organic structure of soil and flora are the harmful outcomes of forest fire on a local level (Chen Z 2006).

The World forest cover encompasses 4000 million hectares or 30.6% of the earth surface according to Global Forest Resources Assessment (FAO 2015). They are the primary environmental assets playing a critical part in preserving the environment's ecological equilibrium. Forest ecosystems have the most important role in natural air cleaning and oxygen synthesis (Pourtaghi et al. 2015).

Forest fires affect around 64% of India's total forest area, resulting to huge economic loss. It can be started naturally (lightning) or artificially (by human actions), however the latter (Joseph et al. 2009) is more common in India accounting to over 90% of forest fires. Although human-caused wildfires are the most prevalent trigger, natural variables such as meteorological conditions and geography play a significant part in their uncontrolled spread. It is critical to identify the sensitive regions that fall inside "forest fire risk zones" in this regard. Thus all the characteristics playing a decisive role towards forest fire must be identified using advanced geospatial technologies in order to plan proper remedial measures.

Geospatial technologies have the ability to provide timely and precise spatial and temporal information for complex fire zone modeling. Further, integrating advanced multi-criteria decision-making (MCDM) models offers an innovative and accurate approach towards fire risk zones assessment (Lamat et al. 2021). Multi-criteria decision analysis (MCDA) models combined with GIS are decisive tools for calculating and forecasting natural and man-made risks (Gigovi'c et al. 2016; Gigovi'c et al. 2017). To handle conflicting preferences among the many criteria, MCDA approaches were devised. The analytical hierarchical process (AHP) is a widely utilized MCDA procedure (Saaty 1980). It is one of the most used MCDMs to successfully detect fire risk zones. AHP enables for the measurement of a decision maker's (DM) consistency in collective decision making as well as the management of qualitative and quantitative criteria. For assessing the comparative relevance of criteria, sub criteria, and substitutes, the AHP technique employs a pair wise generating process. TOPSIS is another MCDA technique given by Hwang and Yoon in 1981, functioning on the principle of shortest distance from the ideal best and longest distance from the ideal worst (Dhanalakshmi et al. 2020).

In recent decades, forest fire hazard analysis based on comprehensive modeling techniques has become indispensable tools for forest fire mitigation. Multi-criteria like fuel, geography, and weather conditions that make up a potential fire habitat are included in the integrated model. The key elements (Lamat et al. 2021) for the forest fire risk assessment include fuel, topographical data (slope, aspect), nearness to highways, and weather conditions (temperature and relative humidity).

With the coming winters, which stretch through December to March, Sikkim's subtropical Sal woods become more prone to flames. Of all of the other forest types, East Himalayan Sal has the greatest danger of forest fires. The Sal Forest and subtropical woodlands had the largest percentage of fire burnt zones, according to satellite imagery (Verma et al. 2017). Forest fires are becoming more common in Sikkim, resulting in forest loss and ecological imbalance. According to Sikkim's forest fire data of 2009, 905 hectares of land were damaged which is increasing with each passing year. According to the research, manmade activities are to be blamed for the majority of forest fires in Sikkim (Sharma et al. 2012).

The slash-and-burn cultivation, known locally as jhum, has a substantial influence in forest fire. It is impertinent to gauge the wildfire risk of the study area being a forest-dominated region. Furthermore, previous to the current study, no such approach or model for detecting fire hotspots of the survey area has been studied. Thus the present study is intended towards helping, developing and implementing suitable strategies to avoid/minimize the loss triggered by forest fires in the West Sikkim district by FFSZ mapping through MCDA techniques.

2. Study Area

West Sikkim is the second biggest district of the northeast hill state of Sikkim in India. The area is enclosed within 27˚ 10'N to 27˚30'N and longitude 87˚50'E to 88˚30'E, having a total area of 1,166 km^2. The elevation in the area varies from 400 to 2500 metres above sea level (MSL). The district has two subdivisions - Gyalshing and Sorreng, encompassing 125 villages. The head office of the district is Geyzing. The average annual rainfall is 1,66,428 mm per month. The maximum mean temperature is 17°C -27°C while the mean minimum temperature is 02°C -10°C. The current population, according to the 2011 census, is 136,435, including 70,238 male and 66,197 female populations (Fig. 1).

3. Materials And Methodology

3.1 Thematic layers generation

“Humidity, elevation, slope, aspect, temperature, rainfall, wind speed, and land use/ land cover” were the parameters employed for forest fire risk zone mapping of the surveyed region. These parameters were collected using earth observation satellite and auxiliary data. Using Landsat – 8 OLI (2021) and supervised classification, a Land Use Land Cover map of the research area was created. Furthermore, a Digital Elevation Model (DEM) derived from the “Advanced Space borne Thermal Emission and Reflection Radiometer (ASTER)” was obtained with a resolution of 30 m from the USGS, Earth Explorer for elevation, slope, and aspect purposes. Meteorological datasets such as temperature, rainfall, humidity, and wind speed for four separate meteorological stations in the district and its surrounding areas were collected from Global Weather data for SWAT. Figure 2 depicts the detailed methodology of the current investigation.

08 factors were used to examine the forest fire danger zone in Sikkim's West Sikkim district - humidity (H), land-use/land-cover (LU/LC), elevation (EL), temperature (TEMP), slope (SL), aspect (AS), wind speed (WS), and rainfall (RF).

3.1.1 Humidity

The research area's humidity map is shown in Fig. 3. When relative humidity surpasses 60%, forest fires are more likely (Malik et al. 2013). Higher temperatures cause forest fuels to dry out faster. As per the “Intergovernmental Panel on Climate Change”, the chief causes of forest fires in Asia include droughts induced by drier weather, a lack of rainfall, an increase in temperature, and a drop in precipitation (Berwyn 2018).

3.1.2 Land-use/Land-cover

Human activities have increased LULC dynamics, resulting in numerous alterations that affect various forests and ecosystems (Nikhil et al. 2021; Tien et al. 2016). Former researches (Vadrevu et al. 2010; Szpakowski et al. 2019) have signified the dominance of land

cover classes in predicting a specific area's danger of fire due to fuel kinds and characteristics. LULC (Fig. 4) has been divided into four categories in this study: forest land, settlement, snow cover, and water body.

3.1.3 Elevation

Forest fires typically decrease with increasing altitude owing to lesser temperatures and increased humidity (Rothermel et al. 1983). The study area's elevation ranges from 500 to 2500 meters, which was divided into four categories: low (> 500 meters), moderate (501–1000 meters), high (1001–1500 meters), and extremely high (1501–2500 meters), as shown in Fig. 5. AHP was used to compute the actual weights of various altitude levels.

3.1.4 Temperature

Temperature plays a vital role in forest fires. High temperatures contribute to the increasing rate of evaporation, fuelling drying of leaves, needles, dead trees, twigs etc creating suitable circumstances for forest fire (Bonora et al. 2013). The research area's border areas (Fig. 6) have a rather high temperature (27˚C).

3.1.5 Slope

The rate at which a fire spreads is influenced by the slope. Fire spreads more rapidly towards the peak than foothills of the mountains (Jaiswal et al. 2002). The slope map (Fig. 7) was categorized into: low (> 15.30), moderate (15430.70), high (30845.70), and very high (< 45.70).

3.1.6 Aspect

A slope facing east absorbs more morning sunshine than one facing west. In the northern hemisphere, a south-facing hill receives more sunshine, resulting in higher temperatures that quickly dry the fuel. This makes wildfires more likely (Mukherjee et al. 2014). North and Northeast (Fig. 8), East and Southeast, South and Southwest, and West and Northwest were the four aspect classes studied.

3.1.7 Wind speed

This parameter has a huge influence on the speed and spread of fire (Bessie et al. 1995; Keeley 2004; Kayet et al. 2020). The average wind speed of the study area is 1,111.32 km/h. The wind speed map was divided into four classes – 1.5–2.8 km/h, 2.81–4.13 km/h, 4.14–5.73 km/h and 5.74-8 km/h. Wind speeds were most high in the lower and medium altitudes, while they were low at the higher altitudes (Fig. 9).

3.1.8. Rainfall

In general precipitation affects natural vegetation, the fuelling elements and soil moisture content (Pereira et al. 2005). Thus, rainy season experienced fewer fire occurrences in West Sikkim district. The research area's average rainfall is 1,66,428 mm per month. Areas situated in the higher altitude had very little ignition and fire spread. The precipitation map was categorized into four grades such as > 60.8 mm, 60.9–90.5 mm, 90.6–130 mm and more than 130 mm. The concentration of precipitation varied across the research region (Fig. 10).

3.2 Weight calculation using AHP

The most significant factor in predicting the forest fire zone is determining the weight of each thematic layer. Fuzzy sets (Bellman 1970), linguistic variables (Chen et al. 1992), and AHP (Saaty et al. 1980) were the most commonly used approaches for computing weightage to identify the fire risk zone. However, according to Vadrevu et al. (2010) and Sharma et al. (2014), the most prevalent method for determining fire risk zones is AHP. Saaty in 1980 created AHP which is a decision-added approach for generating relative ratio scales in paired comparisons. At each hierarchical level, “pair-wise comparison matrixes” were created amongst the various theme levels. To compare all elements against each other depending on their relevance, a “pair-wise comparison matrix” was created (“equal, moderate, strong, very strong, and extremely strong”). All themes and their characteristics were assigned relative level of significance using Saaty's 1–9 scale, where value "1" denotes "equal importance" between the two themes and value "9" denotes "extreme importance" of one theme compared to the other, as shown in Table 1 (Saaty et al. 1980). By dividing each element of the pair-wise matrix by the total of its columns, the normalized relative weight and final weights were determined (Table 2). The primary eigen vector of each criterion's square matrix was used to determine the weights of each layer. Based on their relative relevance, the higher the weights, the larger the influence of the factors on the forest fire. The following formulae were used to compute the weights of each of the theme levels:

$FRSI = H_rH_w + L_rL_w + E_rE_w + T_r T_w + S_rS_w + A_r A_w + W_rW_w + R_rR_w$(1)

In this methodology, where FRSI is Forest Fire Susceptibility Index, H is humidity, L is land-use/land-cover, E is elevation, T is temperature, S is slope, A is aspect, W is wind and R is rainfall. The suffix 'r' and 'w' represent the rank and weight of each layer (Eq. 1). The calculation of Eigen Vector (by Eq. 2), weighting coefficient (by Eq. 3), Eigen value (by Eq. 4), Consistency index (by Eq. 5) and consistency ratio (by Eq. 6) are shown in Table 3. The normalized pair-wise matrix was calculated and shown in Table 4. We use following equations for our calculation.

$$v_p = \sqrt[n]{w_1 * w_{2\ldots} * w_n} \quad (2) \qquad C_P = \frac{v_P}{v_{P_1} + \ldots v_{pn}} \quad (3)$$

$$\lambda_{max} = \frac{E}{n}$$

4

Where,

$w_1, w_{2\ldots} w_n$ are the rating of factors.

n indicates no. of criteria.

Table 1
Scale for a Pair-wise Comparison Matrix

Intensity Importance	Linguistic Variable
1	Equal Importance
2	Equal to moderate importance
3	Moderate importance
4	Moderate to the strong importance
5	Strong importance
6	Strong to the very strong importance
7	Very strong importance
8	Very to the extremely strong importance
9	Extreme importance

Table 2
Normalized and Final Weights of Different Features of Thematic Layer for Assessment of Forest Fire

Thematic layers	Normalized weight (%)	Sub-class	Final Weight
Land-use/land-cover	0.33	Settlement	0.19
		Forest	0.09
		water bodies	0.05
		Snow cover	0.01
Humidity	0.23	> 20	0.13
		21–40	0.06
		41–60	0.03
		< 60	0.01
Elevation (m)	0.15	> 500	0.09
		500–1000	0.04
		1001–1500	0.02
		1500–2500	0.008
Temperature (C)	0.11	> 4.3	0.06
		4.4-8	0.03
		8.1–12.6	0.01
		12.7–17.3	0.006
Slope (degree)	0.07	> 15.3	0.04
		15.4–30.7	0.02
		30.8–45.7	0.008
		< 45.7	0.004
Aspect	0.06	SW, S	0.04
		NW, W	0.02
		E, SE	0.007
		NE, N, Flat	0.003
Wind speed (km/h)	0.04	1.5–2.8	0.02
		2.81–4.13	0.01
		4.14–5.73	0.004
		5.74-8	0.002
Rainfall (mm)	0.02	> 60.8	0.01
		60.9–90.5	0.005
		90.6–130	0.002
		< 130	0.001

Consistency Index (CI) which is a deviance or degree of consistency was calculated using Eq. 2, where CI = Consistency Index, *n* = Number of criteria.

Eq. 3 shows the calculation of Consistency ratio (Cr): where RI = random inconsistency.

$$CI = \frac{\lambda_{\max - n}}{n} (5)$$

$$CR = \frac{CI}{RI} (6)$$

If Consistency ratio (Cr) is ≤ 0.10, then the inconsistency is acceptable. Random inconsistency (RI) values for '*n*' number of criteria, i.e., number of parameters (Saaty et al. 1980) (Table 5). Our calculated Consistency ratio (Cr) is 0.097 i.e. less than 0.01 which indicates the judgement is valid.

Table 3
Pair-wise Comparison Matrix of the Thematic Layers and consistency calculation

	HD	LULC	ELV	TEMP	SL	ASP	WS	RF	v_p	C_P	D = A* C_P	E = D $/C_P$	λmax	CI	CR
HD	1	3	3	5	5	6	7	7	4.00	0.34	3.02	8.94	8.96	0.14	0.0977
LULC	0.33	1	3	4	5	5	6	7	2.83	0.24	2.13	8.90			
ELV	0.33	0.33	1	3	3	4	5	5	1.77	0.15	1.31	8.76			
TEMP	0.2	0.25	0.33	1	3	3	5	6	1.21	0.10	0.91	8.94			
SL	0.2	0.2	0.33	0.33	1	2	3	7	0.81	0.07	0.59	8.69			
ASP	0.17	0.2	0.25	0.33	0.5	1	3	5	0.62	0.05	0.45	8.63			
WS	0.14	0.17	0.2	0.2	0.33	0.33	1	5	0.39	0.03	0.30	9.13			
RF	0.14	0.14	0.2	0.17	0.14	0.2	0.2	1	0.21	0.02	0.17	9.74			
Total	2.51	5.29	8.31	14.03	17.97	21.5	30	43	11.84	1.00	-	71.71			

A = Comparison pairwise matrix (from HD to RF)

Table 4
Normalized Pair-wise Matrix

	HD	LULC	ELV	TEM	SL	ASP	WS	RF	Total.Wgt	Nor.Wgt
HD	0.40	0.57	0.36	0.36	0.28	0.28	0.23	0.16	2.64	0.33
LULC	0.13	0.19	0.36	0.29	0.28	0.23	0.20	0.16	1.84	0.23
ELV	0.13	0.06	0.12	0.21	0.17	0.19	0.17	0.12	1.17	0.15
TEMP	0.08	0.05	0.04	0.07	0.17	0.14	0.17	0.14	0.86	0.11
SL	0.08	0.04	0.04	0.02	0.06	0.09	0.10	0.16	0.59	0.07
ASP	0.07	0.04	0.03	0.02	0.03	0.05	0.10	0.12	0.46	0.06
WS	0.06	0.03	0.02	0.01	0.02	0.02	0.03	0.12	0.33	0.04
RF	0.06	0.03	0.02	0.01	0.01	0.01	0.01	0.02	0.17	0.02

Table 5
Random Inconsistency (RI) Values

n	2	3	4	5	6	7	8	9
RI	0	0.52	0.9	1.12	1.24	1.32	1.41	1.45

3.3. Assessment of TOPSIS model in forest fire mapping: TOPSIS is a multi-criteria decision-making model which determines the dissimilarity from the ideal solution, introduced by Hwang and Yoon in 1981. The principle of this method is to figure out the best option which has shortest distance from ideal solution and longest distance from worst solution. The indicators value lies between 0 and 1 in which nearest to 1 signifies higher weightage i.e. most susceptible for forest fire in our case and vice versa (Tali et al. 2016). The calculation of TOPSIS was done in the following manner:

1. To Find the vector data normalization ($\bar{X}_{ij}$) we use Eq. no……7 and the outcomes are represented in Table 6.

$$\bar{X}_{ij} = \frac{X_{ij}}{\sqrt{\sum_{i=1}^{n} X_{ij}^2}} \quad (7)$$

2. To calculate the weightage Normalized matrix(V_{ij}), the results of normalized matrix ($\bar{X}_{ij}$) are multiplied by the weightage. (Table 7)

$$V_{ij} = \bar{X}_{ij} \times W_j \quad (8)$$

3. Based on Geographical knowledge and referencing literatures the ideal best (V_j^+) and ideal worst (V_j^-) values are determined.

4. Euclidean distance S_i^+ between each criterion and ideal best (V_j^+) is being calculated by applying Eq. no. 9.

$$S_i^+ = \left[\sum_{j=1}^{m} \left(V_{ij} - V_j^+\right)^2\right]^{0.5} \quad (9)$$

5. Euclidean distance S_i^- between each criterion and ideal worst (V_j^-) as

$$S_i^- = \left[\sum_{j=1}^{m} \left(V_{ij} - V_j^-\right)^2\right]^{0.5}$$

10

6. And finally, Performance Score P_i is calculated and after that the score in plotted using IDW technique that are classified into 5 categories by applying Eq. no. 8 and the Performance score are shown in Table 8.

$$P_i = \frac{S_i^-}{S_i^+ + S_i^-}$$

11

Table 6
Calculation of Normalized Matrix

#	Latitude	Longitude	LULC	Humidity	Elevation	Temperature	Slope	Aspect	Wind Velocity	Rainfall
S1	88.13	27.34	0.0003	0.0038	0.1398	0.0008	0.0009	0.0000	0.0001	0.0009
S2	88.14	27.23	0.0003	0.0039	0.1398	0.0008	0.0005	0.0000	0.0000	0.0009
S3	88.29	27.35	0.0004	0.0048	0.1398	0.0009	0.0009	0.0001	0.0001	0.0010
S4	88.20	27.57	0.0003	0.0017	0.1400	0.0004	0.0006	0.0000	0.0000	0.0004
S5	88.29	27.19	0.0004	0.0117	0.1389	0.0022	0.0018	0.0001	0.0002	0.0022
.....										
S496	88.28	27.34	0.0002	0.0051	0.1398	0.0010	0.0006	0.0001	0.0001	0.0010
S497	88.31	27.40	0.0002	0.0045	0.1397	0.0010	0.0009	0.0001	0.0001	0.0012
S498	88.33	27.39	0.0005	0.0059	0.1395	0.0013	0.0028	0.0002	0.0002	0.0014
S499	88.12	27.42	0.0003	0.0018	0.1399	0.0004	0.0006	0.0001	0.0001	0.0005
S500	88.11	27.53	0.0003	0.0018	0.1400	0.0004	0.0002	0.0001	0.0000	0.0005

Table 7: Calculation of Weighted Normalized Matrix

#	Latitude	Longitude	LULC	Humidity	Elevation	Temperature	Slope	Aspect	Wind Velocity	Rainfall
S1	88.13	27.34	0.0009	0.0166	0.9987	0.0075	0.0125	0.0005	0.0020	0.0466
S2	88.14	27.23	0.0009	0.0171	0.9988	0.0077	0.0067	0.0004	0.0009	0.0448
S3	88.29	27.35	0.0011	0.0207	0.9985	0.0086	0.0129	0.0011	0.0026	0.0489
S4	88.20	27.57	0.0009	0.0073	0.9997	0.0034	0.0080	0.0004	0.0011	0.0219
S5	88.29	27.19	0.0012	0.0508	0.9921	0.0199	0.0262	0.0024	0.0042	0.1098
.....										
S496	88.28	27.34	0.0006	0.0220	0.9984	0.0090	0.0084	0.0011	0.0027	0.0506
S497	88.31	27.40	0.0006	0.0194	0.9979	0.0090	0.0126	0.0023	0.0032	0.0591
S498	88.33	27.39	0.0015	0.0257	0.9963	0.0114	0.0394	0.0029	0.0038	0.0712
S499	88.12	27.42	0.0010	0.0078	0.9996	0.0038	0.0085	0.0010	0.0013	0.0255
S500	88.11	27.53	0.0009	0.0079	0.9997	0.0037	0.0027	0.0009	0.0012	0.0238

Table 8
Calculation for Euclidean distance S_i^+and Performance Score (P_i)

#	Latitude	Longitude	S_i^+	S_i^-	PERFORMANCE SCORE (P_i)
S1	88.13	27.34	0.19	0.44	0.69
S2	88.14	27.23	0.20	0.43	0.67
S3	88.29	27.35	0.15	0.47	0.75
S4	88.20	27.57	0.48	0.14	0.23
S5	88.29	27.19	0.05	0.59	0.91
....					
S496	88.28	27.34	0.14	0.48	0.76
S497	88.31	27.40	0.14	0.49	0.77
S498	88.33	27.39	0.10	0.53	0.83
S499	88.12	27.42	0.42	0.21	0.33
S500	88.11	27.53	0.44	0.19	0.30

4. Results And Discussion

Forest fires are a typical occurrence in the research region. A secondary data source using 194 wildfire locations from Sikkim State Disaster Management Authority (SSDMA) shows approximately 1132.55 hectares of area have been damaged by forest fire incidence between the years 2004-20 (Table 9) and maximum number of incidences occurred in the Sal forests (*Shorearobusta*) and ground bushes (Table 10).

Table 9
Block-wise total Incidences and Area damage (2004–2020), West Sikkim District

Block name	Incidence (no)	Area damage (ha)
Gyalshing	98	703.33
Sorreng	67	429.22

MCDM techniques of AHP and TOPSIS approach were employed for forest fire risk mapping. The data was converted to raster format and tallied with a raster calculator in ArcGIS software to outline the forest fire potential risk zone after computing the ultimate weights of all parameters. To minimize pixel speckling, the map was additionally refined in ArcGIS using a majority filter. The result of TOPSIS and AHP shows spatial differentiation of various susceptibility risk zonation. By our indexing terms, “Very High Zone” of AHP spreads dispersedly and is mostly concentrated along the south-eastern and south-western parts of the study area. As per the susceptibility risk zonation according to TOPSIS, the “Very high zone” was found to be concentrated only along the south-eastern part. TOPSIS analysis carved out almost 29.94% area (348.499 km^2) of West Sikkim under Very High fire Susceptibility Zone compared to AHP (13.06% or 152.331 km^2). The differentiation between the results of two applied MCDM is more pronounced in the “Moderate Susceptibility Zone”, where susceptibility was 29.94% of area in case of AHP while it was 15.94% in case of TOPSIS (Table 11).

Table 10
Major Species Damaged by Forest Fires (2004–2020) in West Sikkim

Sl. No	Local Name	Scientific Name	No of incidence
1	Teak	Tectonagrandis	8
2	Sal	Shorearobusta	51
3	Simal	Bombaxceiba	4
4	DhalneyKatus	Castanpsisindica	6
5	Ground bushes		72
6	Junifer	Juniperusrecurva	3
7	Bamboo	Bambuseae	9
8	Mauwa	Engelhardtiaspicata	4
9	Chewri	Bassiabutyracea	5
10	Chirpine	Pinusroxburghii	3

The spatial result of AHP and TOPSIS is showing some difference. However in both the MDCM models the concentration of “Very high Susceptibility Zone” is found in the south-eastern part of our study area. This corroborates with the forest fire incidents occurring from 2004 to 2019 which were recorded in the same area (Fig. 11.1 and Fig. 11.2). The high humidity (> 60%) (Fig. 3), low elevated zone, high temperature (8.1^0 C to 12.6^0C) (Fig. 6), precipitation < 90 mm (Fig. 10) enhances the chances of forest fire incidents in that region. The northern section of the region falls under very low susceptibility zone (in both MCDM models) which again is substantiated by the minimal fire incidents in this zone. This is due to its location in highly elevated zone (> 1500 m) causing snow fall (Fig. 4) as well as low temperature (< 4.3^0C) (Fig. 6), and having low to moderate humidity (20 to 40%) (Fig. 3). Forest fire risk was highest in the sparsely populated areas and was centered primarily in the district's south-eastern part, where agriculture (mostly slash and burn) was widely practiced. Slash and burn agriculture is a major driving force behind the region’s forest fires. The majority of fires were started by humans when a source of ignition, such as a bare flame, cigarette, electric spark, or any other source of ignition, came into contact with combustible material. The bulk of forest fires have happened in places where people live, followed by forest, water bodies, and only a few have occurred in snow cover across the entire region (Fig. 4). The fire was mostly visible in places with low to moderate elevations (1530 m), as much of the forest cover was found on those slopes, particularly in the research area's southern region (Fig. 11.1). Regions (Fig. 6) having low temperature areas very rarely experienced forest fires owing to moisture content in the fuelling elements. Forest fires were found to be more prevalent in the lower and intermediate elevation ranges of the research region, with

lesser fire occurrences happening at higher altitudes. This is owing to the high humidity of the plant and soil, making the ignition and spread of fire difficult.

Table 11: Distribution of the Forest Fire Susceptible Zone

Fire Susceptible Zone	Color	AHP		TOPSIS	
		Area (km^2)	Percentage (%)	Area (km^2)	% of Area
Very High		152.331	13.062	348.499	29.937
High		282.691	24.241	317.728	27.367
Moderate		349.224	29.946	180.959	15.946
Low		266.593	22.86	180.887	15.105
Very Low		115.351	9.891	139.436	11.644

Validation of Forest Fire Susceptible Map

Overlaying forest fire sites with susceptibility maps is a useful and accurate approach for verifying forest fire susceptibility maps. Between 2004 and 2021, 194 location data of forest fire were obtained from the Sikkim State Disaster Management database. The current forest fire location records were overlapped with the susceptibility maps. This is because the most accurate indicator of consistency and applicability is the similarity of determined findings and actual data state. Figure 11.1 and 11.2 shows the forest fire overlay maps of AHP and TOPSIS susceptibility ratings. It Is seen that about 83% of the forest fire locations fall under high to very high susceptible zone in case of AHP mapping while about 92% of the locations fall under the same category in case of TOPSIS modeling.

The accuracy of the fire risk maps was assessed using the receiver operating characteristic (ROC) curve (Nikhil et al 2021). The area under the curve (AUC) was determined in addition to the ROC curve to see if the model can accurately predict the occurrence of forest fires. The AUC values range from 0 to 1, with 1 signifying the highest level of precision that the model can attain. Models with AUC values of less than 0.5 should be avoided, whereas the acceptability limit for models with AUC values of more than 0.5 varies (Hosmer and Lemeshow 2000). If AUC value is larger than 0.80, according to Das (2020), it implies very accurate models, rendering the mapping acceptable.

The ROC curve for AHP had an AUC value of 76.25 (Fig. 12), indicating it comes within acceptable limit. The AUC value of TOPSIS (Fig. 13) model came to 82.28%. Thus, it can be said that TOPSIS's result is more accurate than AHP as allover 90% of ground data (Forest fire points) spatially fall on "Very High Susceptibility Zone" of TOPSIS (Table 11).

5. Conclusions

Forest fires occurring often and uncontrollably, harm not only forest resources and ecology but also hamper the environment. The Himalayan region is a biodiversity hotspot with low human density, making it susceptible to anthropogenic disturbances like wildfires. The Analytical Hierarchical Process (AHP) and TOPSIS were used to predict wildfire susceptibility zones utilising eight elements determining wildfire occurrence. The final fire risk map was classified into five zones as "very high, high, medium, low and very low vulnerability". Both AHP and TOPSIS showed high performance in both the training and validation datasets with an overall accuracy (AUC-73.25% and 82.28% in case of AHP and TOPSIS respectively) for wildfire vulnerability mapping in the region. In our study it is proved that TOPSIS is much more reliable and much more accurate technique than AHP. So, it can be utilized to any other relevant works for better and accurate result. The overall spatial forest fire location points fall on the "Very High and High zones" of our maps which proves that MCDM is much more valid in this type of study and the parameter selection of forest fire study is also acceptable. A fire risk map is useful for preventing possible disasters caused by flames caused by human activity. It should be beneficial to the Forest Service since a fire risk zone map would allow officials to build up enough fire-fighting infrastructure in regions that are more vulnerable to fire damage. Such kind of susceptibility mapping will save lives, natural resources and property. The prepared maps will guide the authorities to set up proper plans that will be beneficial to minimize the risk or damages of forest fire. It can be done by installing fire watch towers in appropriate locations of "Very high Susceptibility Zone" that helps to reduce expenses of government's fund. The prepared maps can also be useful to scientists, municipal officers, officers of disaster management, local government of the concerned area for early detection of forest fire and manage to prevent it extends higher altitudes, restocking seedlings which has very high burning probability.

Declarations

Competing Interests:

The authors declare no competing interest. The authors have not received any form of funds for this work

References

1. Aliani H, Motlagh MG, Danesh G. et al. (2021) Land suitability analysis for urban development using TOPSIS, WLC and ANP techniques (Eastern cities of Gilan-Iran). Arab J Geosci 14, 1276. https://doi.org/10.1007/s12517-021-07606-1
2. Bessie WC, Johnson EA (1995) The relative importance of fuels and weather on fire behavior in subalpine forests. Ecology 76(3): 747–762.
3. Bonora L, Conese C, Marchi E. et al (2013) Wildfire occurrence: integrated model for risk analysis and operative suppression aspects management. Am J Plant Sci 4(3A):705–710. doi:10.1007/s42452-021-04391-0.
4. Borrelli P, Robinson DA, Fleischer LR. et al (2017) An assessment of the global impact of 21st century land use change on soil erosion. Nat Commun 8(1). https://doi.org/10.1038/s41467-017-02142-7.
5. Chen SJ, Hwang CL (1992) Fuzzy multiple attribute decision making: methods and applications. Springer, NY.http://dx.doi.org/10.1007/978-3-642-46768-4.
6. Chen Z (2006) Effects of fire on major forest ecosystem processes: an overview. J. of Applied Ecology 17(9):1726–1732.
7. Dhanalakshmi CS, Madhu P, Karthick A. et al (2020) A comprehensive MCDM-based approach using TOPSIS and EDAS as an auxiliary tool for pyrolysis material selection and its application. Biomass Conv. Bioref. https://doi.org/10.1007/s13399-020-01009-0
8. Chuvieco E, Salas J (1996) Mapping the spatial distribution of forest fire danger using GIS. International Journal of Geographical Information Systems, 10(3): 333–345, doi: 10.1080/02693799608902082.
9. Forest Survey of India (2003) State of forest report 2003. Ministry of Environment, Forest and Climate Change. http://www.fsi.nic.in/sfr2003.
10. Ganteaume A, Camia A, Jappiot M, San-Miguel-Ayanz J, Long-Fournel M, Lampin C (2013) A review of the main driving factors of forest fire ignition over Europe. Environ Manag 51(3): 651–662. https://doi.org/10.1007/s00267-012-9961-z.
11. Gigovi´c L, Pamu˘car D, Baji´c Z, Drobnjak S (2017) Application of GIS-interval rough AHP methodology for flood hazard mapping in urban areas. Water 9(6):360. https://doi.org/10.3390/w9060360
12. Gigovi´c L, Pamu˘car D, Luki´c D, Markovi´c S (2016) GIS-Fuzzy DEMATEL MCDA model for the evaluation of the sites for ecotourism development: A case study of “Dunavski klju˘c” region, Serbia. Land Use Policy 58: 348–365. https://doi.org/10.1016/j.landusepol.2016.07.030.
13. Hosmer DW and Lemeshow S (2000). Applied Logistic Regression Analysis, Second Edition, John Wiley and Sons Inc., New York.
14. Jaiswal RK, Mukherjee S, Raju KD, Saxena R (2002) Forest fire risk zone mapping from satellite imagery and GIS. International Journal of Applied Earth Observation and Geoinformation 4: 1–10. https://doi.org/10.1080/19475705.2020.1853251.
15. Joseph S, Anitha K, Murthy MSR (2009) Forest fire in India: a review of the knowledge base. J For Res 14: 127–134. https://link.springer.com/article/10.1007/s10310-009-0116-x.
16. Narayan Kayet, N. Kayet, Abhisek Chakrabarty, A. Chakrabarty, Khanindra Pathak, K. Pathak, Satiprasad Sahoo, S. Sahoo, Tanmoy Dutta, T. Dutta, & Bijoy Krishna Hatai, B. Krishna Hatai. (2020). Comparative analysis of multi-criteria probabilistic FR and AHP models for forest fire risk (FFR) mapping in Melghat Tiger Reserve (MTR) forest. Journal of forestry research, 31: 565–579. doi: 10.1007/s11676-018-0826-z
17. Keeley Jon E. (2004) Impact of antecedent climate on fire regimes in coastal California*. International Journal of Wildland Fire 13: 173–182. https://doi.org/10.1071/WF03037
18. Lamat R, Kumar M, Kundu A. et al (2021) Forest fire risk mapping using analytical hierarchy process (AHP) and earth observation datasets: a case study in the mountainous terrain of Northeast India. SN Appl. Sci. 3(425). https://doi.org/10.1007/s42452-021-04391-0.
19. Lentile, L. B., Holden, Z. A., Smith, A. M. S., Falkowski, M. J., Hudak, A. T., Morgan, P., Lewis, S. A., Gessler, P. E., & Benson, N. C. (2006). Remote sensing techniques to assess active fire characteristics and post-fire effects. International Journal of Wildland

Fire, 15(3): 319–345. https://doi.org/10.1071/WF05097.

20. Mandal, T., Saha, S., Das, J. et al. (2022) Groundwater depletion susceptibility zonation using TOPSIS model in Bhagirathi river basin, India. Model. Earth Syst. Environ. 8: 1711–1731. https://doi.org/10.1007/s40808-021-01176-7
21. Malik T, Rabbani G, & Farooq M (2013). Forest fire risk zonation using remote sensing and GIS technology in Kansrao Forest Range of Rajaji National Park, Uttarakhand, India. Inter. J. of advanced RS and GIS, 2(1):86–95.http://technical.cloudjournals.com/index.php/IJARSG/article/view/Tech-56
22. Mikhaylov A, Moiseev N, Aleshin K and Burkhardt T (2020) Global climate change and greenhouse effect, Entrepreneurship and Sustainability Issues, 7, (4): 2897–2913.
23. Mukherjee S, Raj K (2014) Analysis of forest fire of Meghalaya using geospatial tools. In: 15th ESRI India user conference 2014. https://www.esri.in/~/media /esri-india /files /pdfs/event s/uc201 4/proceeding s/paper s/UCP00 53.pdf
24. Nikhil S, Danumah JH, Saha S, Prasad MK, Rajaneesh A, Mammen PC, Ajin R, & Kuriakose SL (2021) Application of GIS and AHP Method in Forest Fire Risk Zone Mapping: a Study of the Parambikulam Tiger Reserve, Kerala, India. J Geovis spat anal 5(14). https://doi.org/10.1007/s41651-021-00082-x
25. Pereira MG, Trigo RM, da Camara CC, Pereira JMC, Leite SM (2005) Synoptic patterns associated with large summer forest fires in Portugal. Agri Forest Meteorology 129(1–2), 11–25. https://doi.org/10.1016/j.agrformet.2004.12.007
26. Pourtaghi ZS, Pourghasemi HR, and Rossi M (2015) Forest fire susceptibility mapping in the Minudasht forests, Golestan province, Iran. Environ Earth Sci 73: 1515–1533. https://doi.org/10.1007/s12665-014-3502-4.
27. Xu R, Yu P, Abramson MJ, Johnston FH, Samet JM, Bell ML, Haines A, Ebi KL, Li S, Guo Y. (2020) Wildfires, Global Climate Change, and Human Health. N Engl J Med. 383(22):2173–2181. doi: 10.1056/NEJMsr2028985.
28. Rothermel RC (1983) How to predict the spread and intensity of forest and range fires. General Technical Report INT-GTR-143. Ogden, UT: USDA Forest Service, Intermountain Forest and Range Experiment Station, 161.
29. Saaty TL (1980) The Analytic Hierarchy Process. McGraw-Hill, New York.
30. Sannigrahi S, Pilla F, Basu B, et al. (2020) Examining the effects of forest fire on terrestrial carbon emission and ecosystem production in India using remote sensing approaches. The Science of the Total Environment. 725:138331. https://doi.org/10.1016/j.scitotenv.2020.138331.
31. Sharma RK, Sharma N, Shrestha DG, et al. (2012) Study of forest fires in sikkim himalayas, india using remote sensing and gis techniques. Arrawatia M, Tambe S (eds.), Climate Change in Sikkim — Patterns, Impacts and Initiatives. 233–244
32. Szpakowski DM, Jensen JLR (2019). A review of the applications of remote sensing in fire ecology. Remote Sens 11(22):1–31.
33. Tali MG, Naeimi A, Esfandiari M (2016). Physical development of Arak city applying natural indicators. Eur J Geogr 7(3):99–110.
34. Vadrevu KP, Eaturu A,, Badarinath KVS. (2010). Fire risk evaluation using multi-criteria analysis—a case study. Environ Monit Assess 166: 223–239. https://doi.org/10.1007/s10661-009-0997-3.
35. Verma S, Singh D, Mani S. et al. (2017) Effect of forest fire on tree diversity and regeneration potential in a tropical dry deciduous forest of Mudumalai Tiger Reserve, Western Ghats, India. Ecol Process 6, 32. https://doi.org/10.1186/s13717-017-0098-0.

Figures

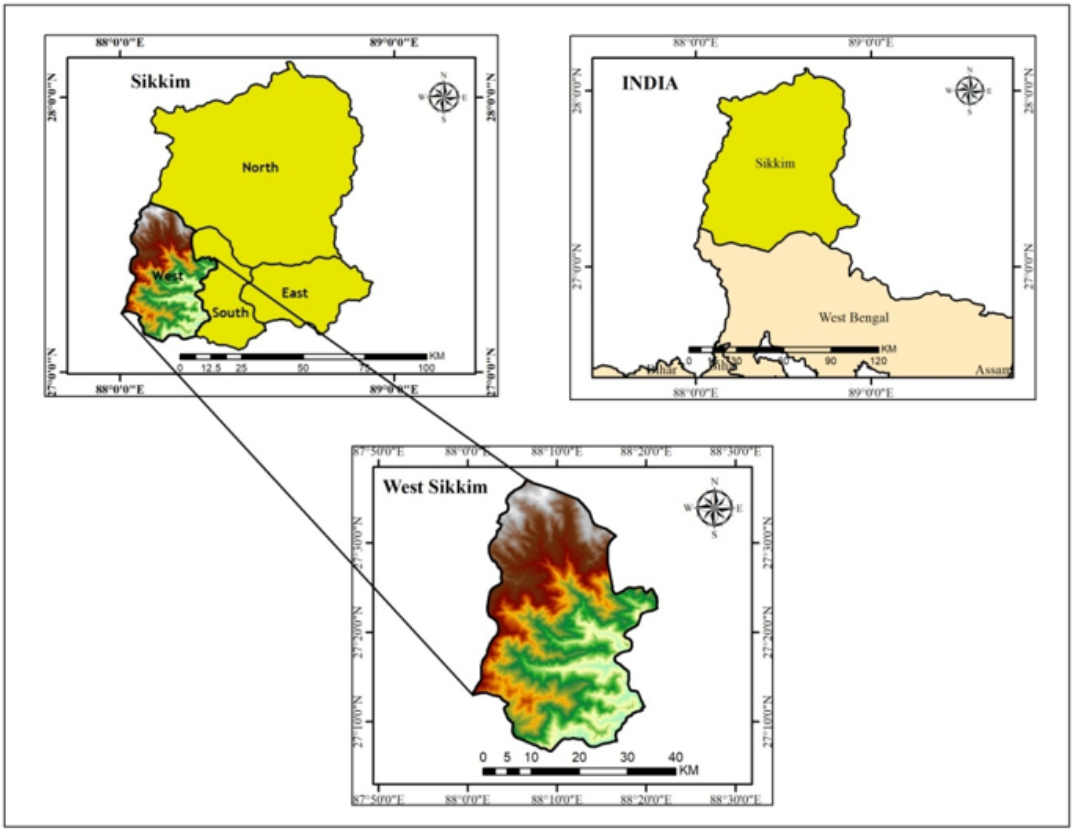

Figure 1

Legend not included with this version

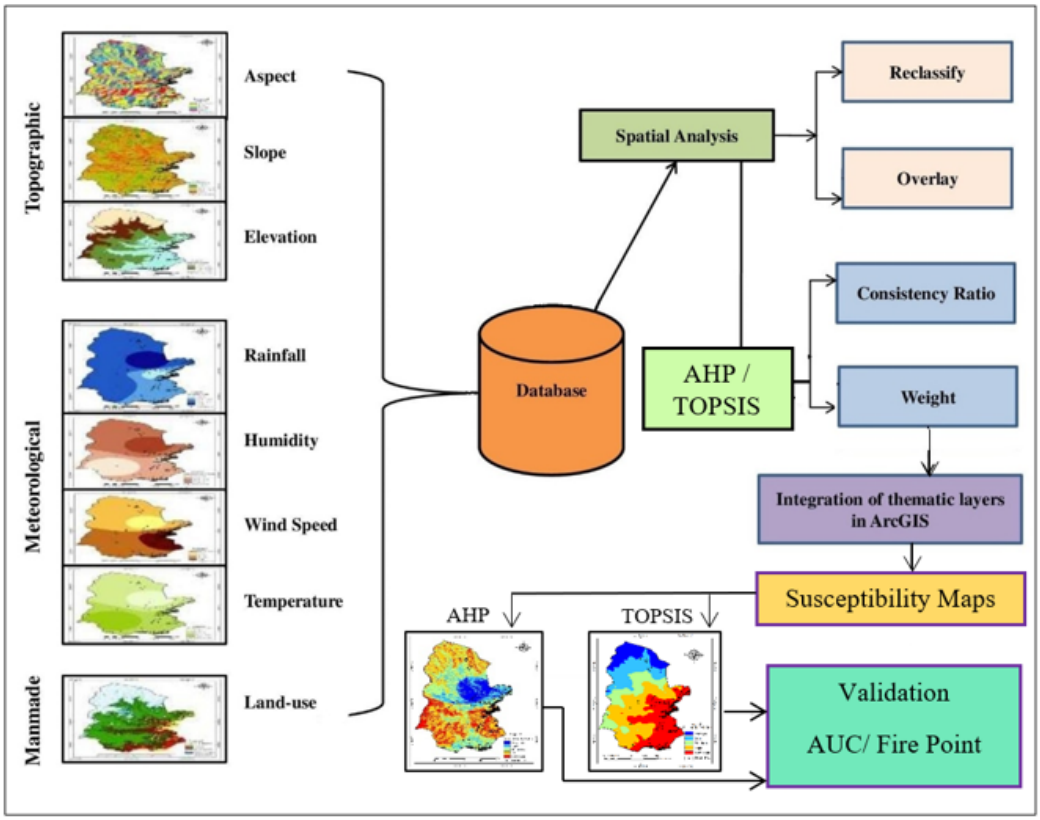

Figure 2

Flow Chart of Methodology

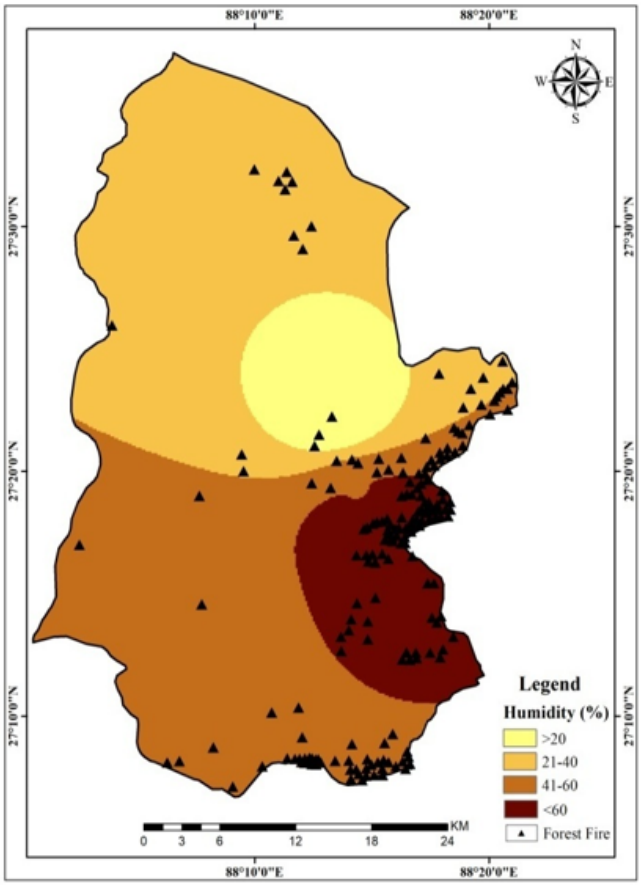

Figure 3

Humidity Map

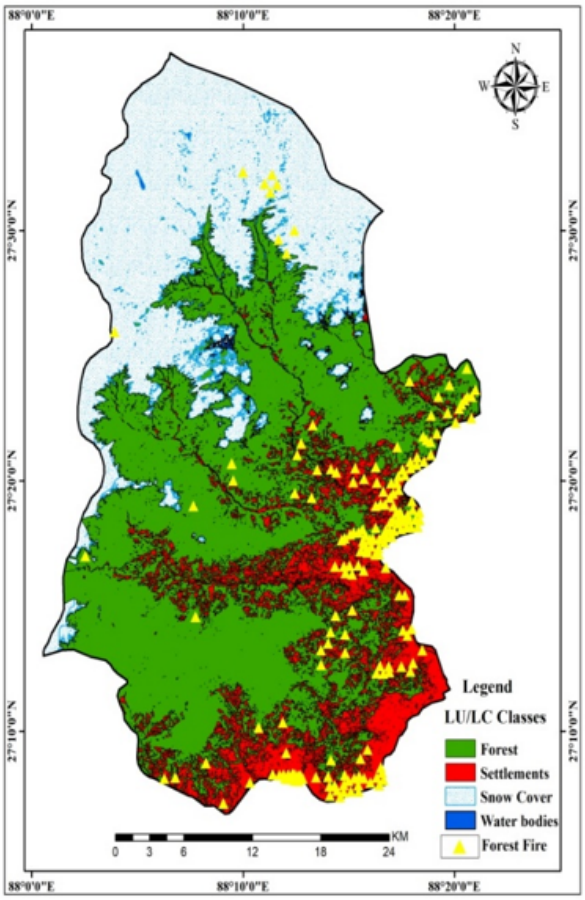

Figure 4

Land-Use/ Land-Cover Map

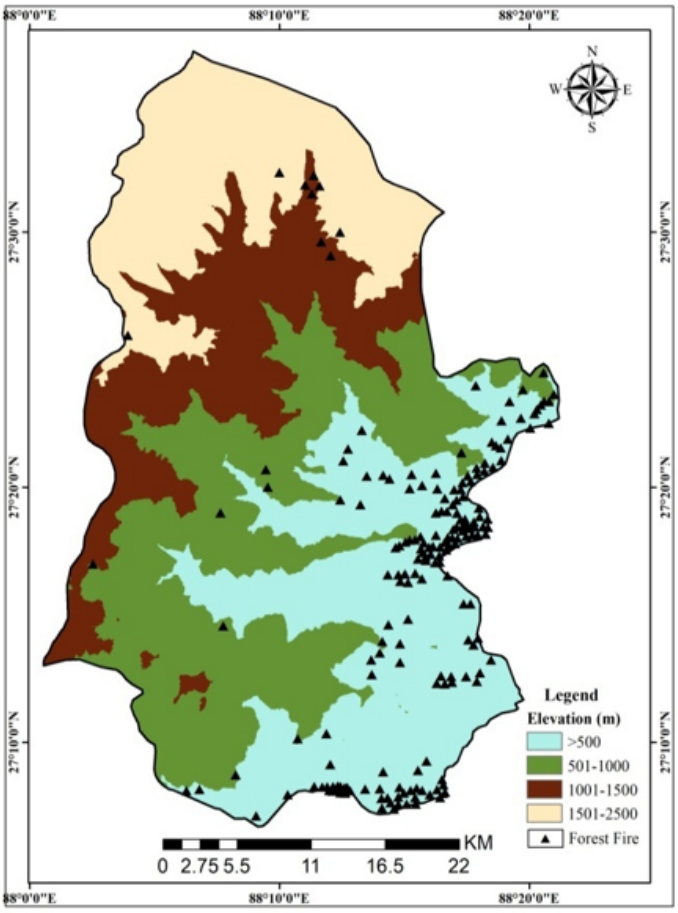

Figure 5

Elevation Map

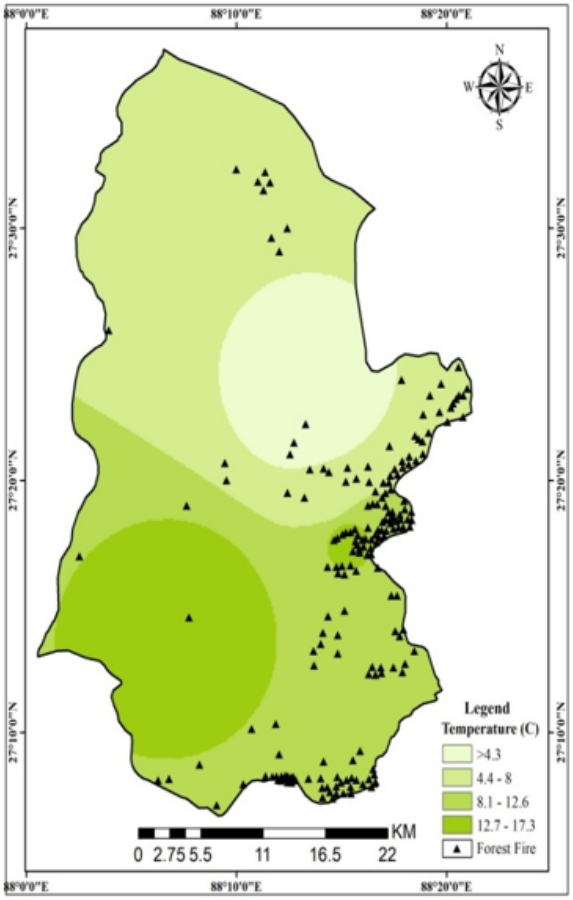

Figure 6

Temperature Map

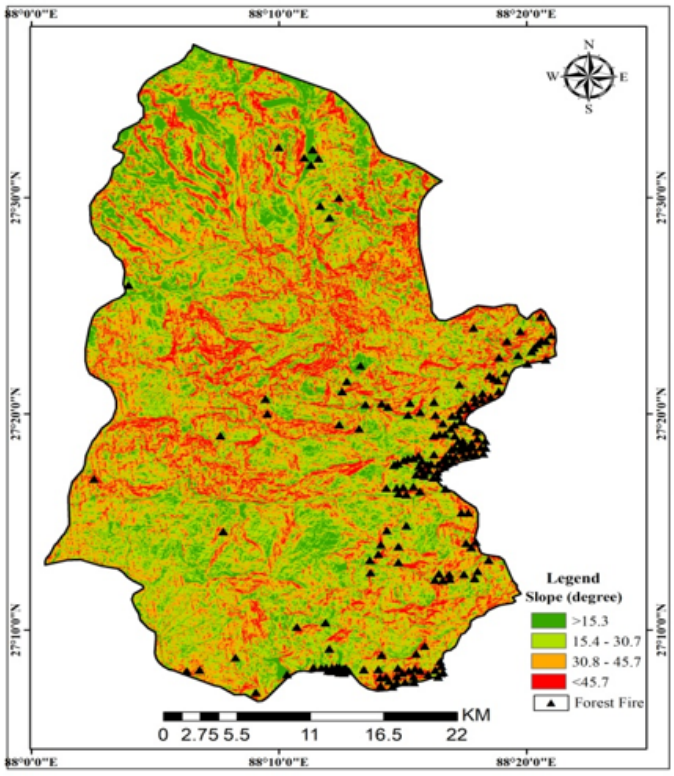

Figure 7

Slope Map

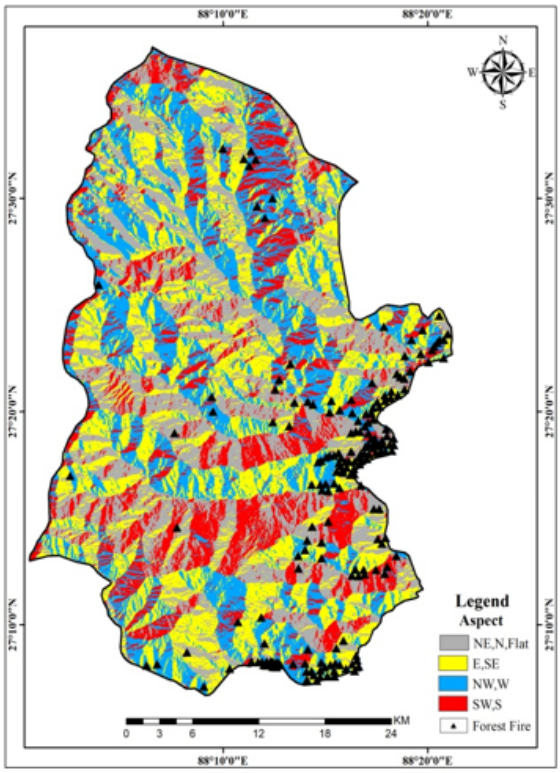

Figure 8

Aspect Map

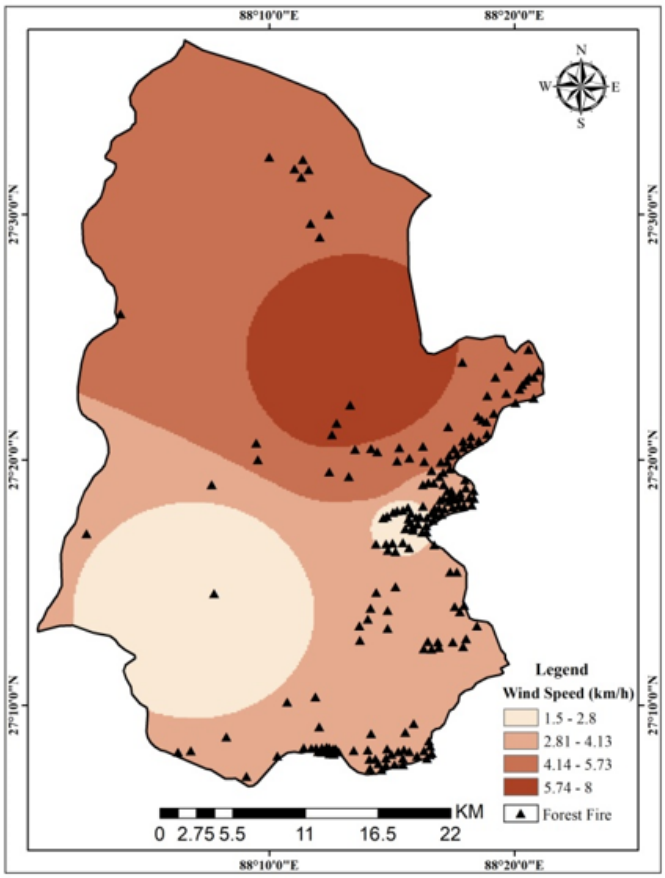

Figure 9

Wind Speed Map

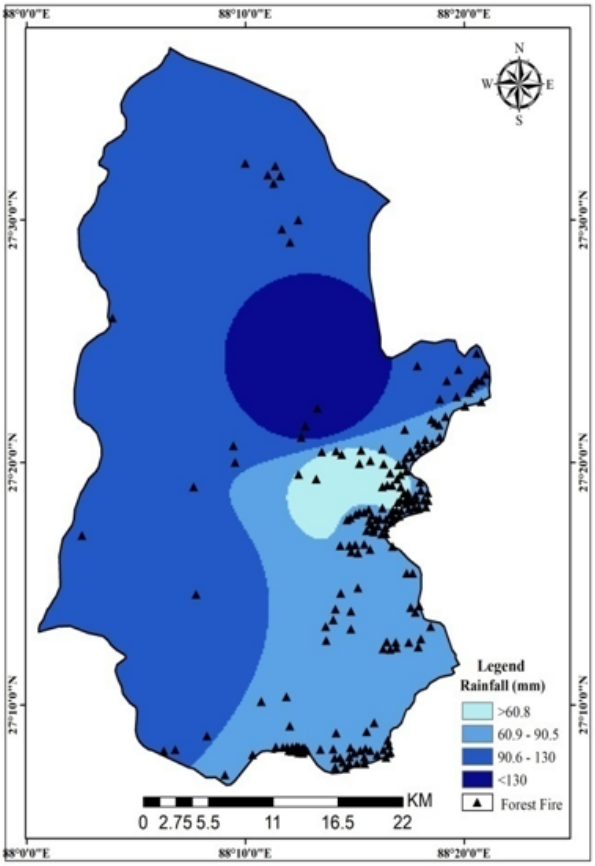

Figure 10

Rainfall Map

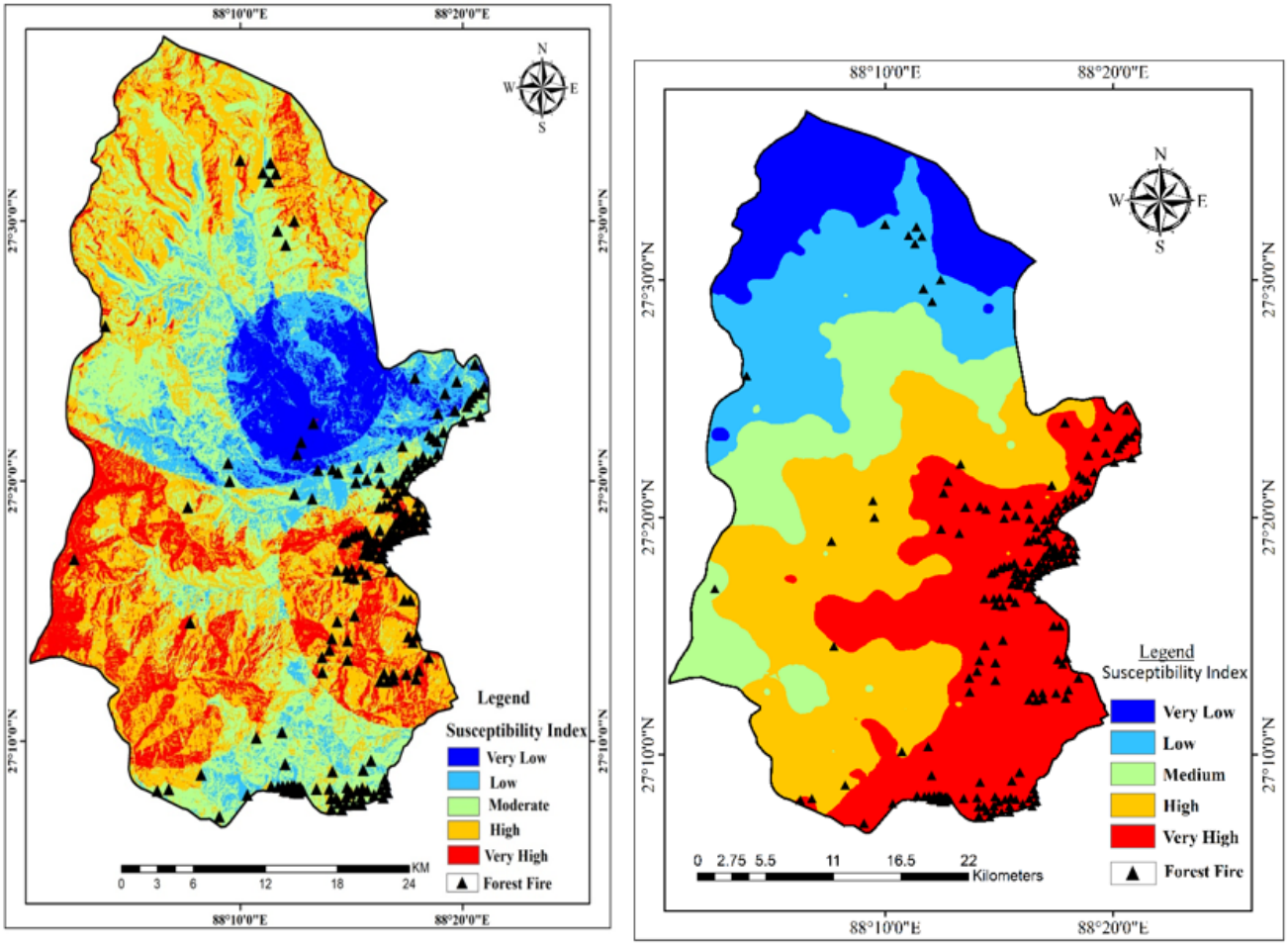

Figure 11

11.1 Forest Fire Susceptibility Map Using AHP. 11.2 Forest Fire Susceptibility Map Using TOPSIS

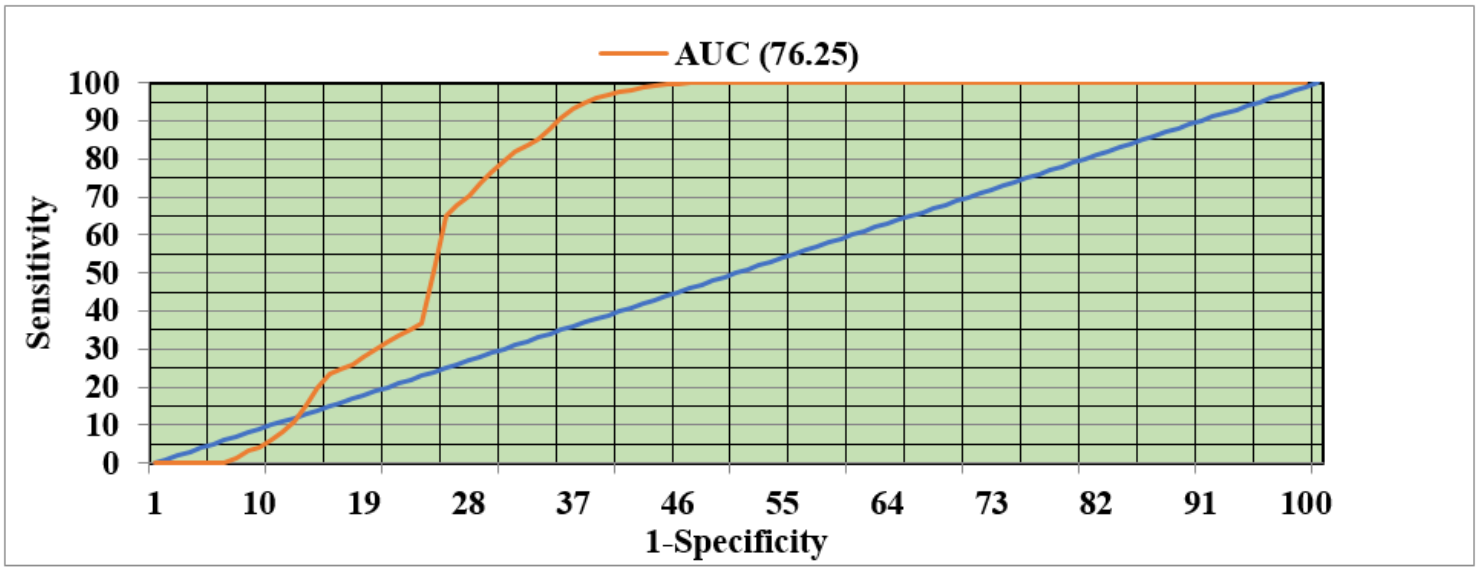

Figure 12

ROC Curve and AUC Value of AHP

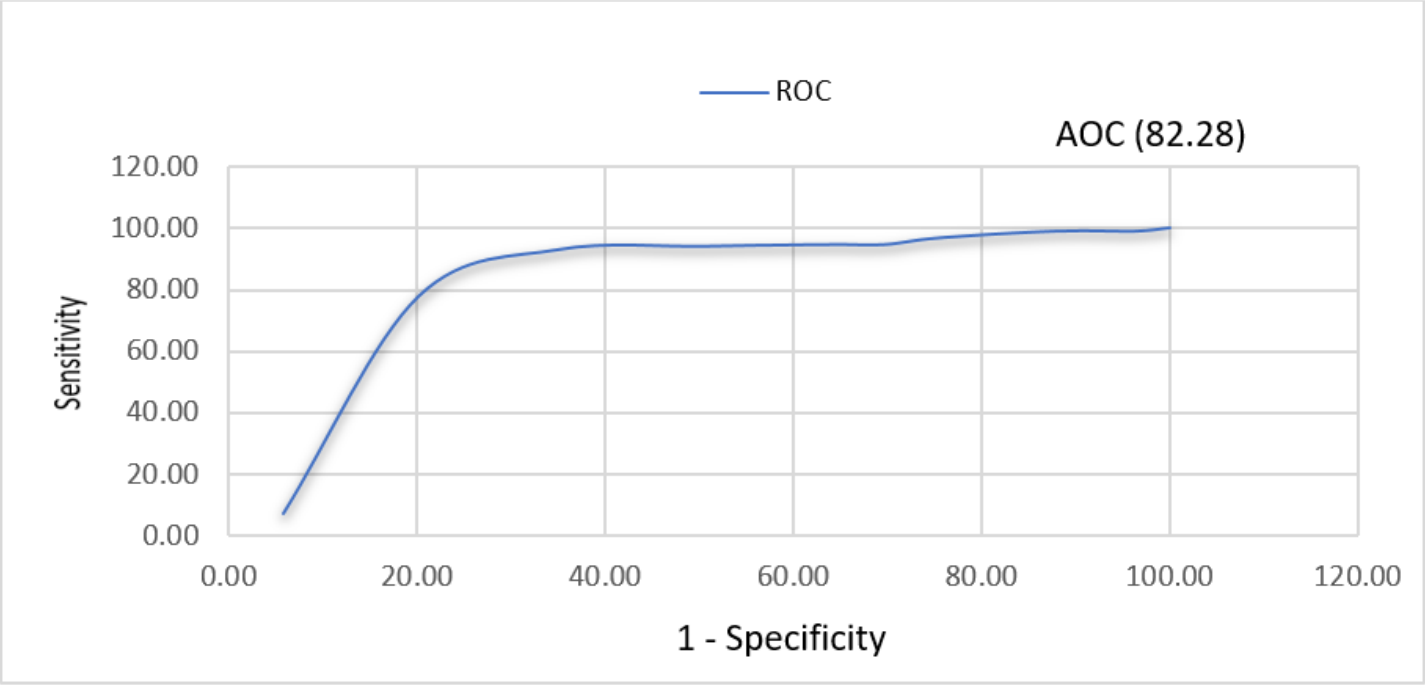

Figure 13

ROC Curve and AUC Value of TOPSIS